Guanidine-modified cellulose enhances capturing and recovery of phosphates from wastewater

Gunanka Hazarika,[a] Sribash Das,[b] Anjali Patel,[a] and Debasis Manna*[ab]

[a]Centre for the Environment, Indian Institute of Technology Guwahati, Assam-781039, India, E-mail: dmanna@iitg.ac.in.

[b]Department of Chemistry, Indian Institute of Technology Guwahati Assam-781039, India,

1. General information:

Each experiment was repeated three times, and the error bars in the figures represent the standard deviations of these repetitions. In the Fourier Transform Infrared Spectroscopy (FT-IR) spectra analysis, sharp peaks are denoted as "s," and broad peaks are marked as "br." The phosphate adsorption experimental procedure involves performing batch experiments in 10 mL glass vials.

2. Synthesis of the polymers:

2.1. Synthesis of compound 1 — First, NaOH (40 mL of 1M aq. solution) was slowly added into the suspension of cellulose (Sigma Aldrich) in water (100 g of a 1 wt %) under stirring conditions at 0 °C. Subsequently, epichlorohydrin (678 µL; excess) was gradually added to the reaction mixture and stirred for 3 h at 60 °C. After that, the reaction mixture was cooled down to room temperature, and the precipitate was collected through centrifugation at 6000 rpm for 10 min, followed by filtration. The resulting precipitate was thoroughly rinsed with deionized water multiple times to eliminate any remaining impurities from the reaction mixture and kept in the oven to dry (Scheme S1).[1, 2] **Characterization of the compound:** solid-state FT-IR (cm^{-1}) = 901 (s), 1054-1036 (s), 1161-1104 (s), 1223 (s), 1372 (s), 1437 (s), 1626 (s), 2903 (br), and 3334 – 3283 (br).

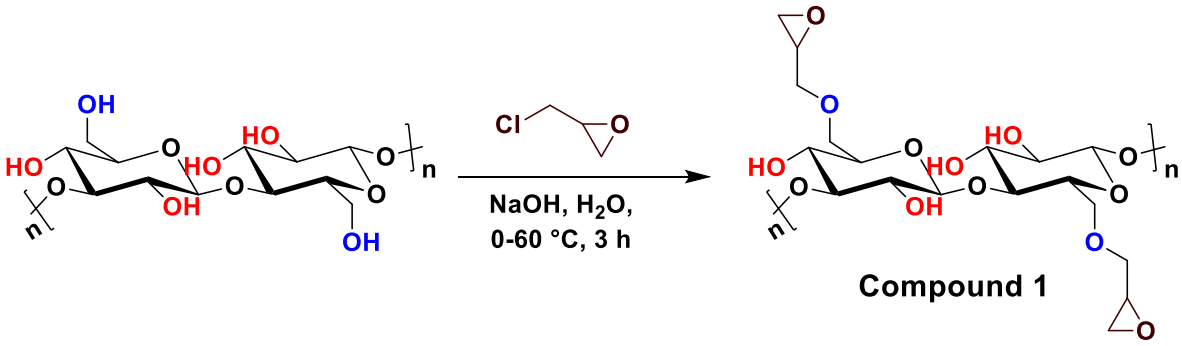

Scheme S1. Synthesis of epoxy-modified cellulose (compound **1**).

2.2. Synthesis of gCP —1-Aminoguanidinium hydrogen carbonate (1.6 g) was dissolved in water, and the pH of the solution was adjusted to 12 by adding NaOH. The mixture was stirred for 15 min at room temperature. Subsequently, this solution was slowly added to the suspension of compound **1** (100 g, 1 wt%) in water while being subjected to stirring at 0 °C. The temperature of the reaction mixture was then increased to 60 °C and stirred for another 3 h. Afterwards, the reaction mixture was allowed to cool down to room temperature, and the resulting solid was separated by centrifugation at 6000 rpm for 10 min, followed by filtration.

The collected solid was thoroughly washed with deionized water multiple times to eliminate any remaining impurities from the reaction mixture, and it was then dried in an oven (Scheme S2).[1, 2] **Characterization of the compound:** solid-state FT-IR (cm^{-1}) = 1017 (s), 1111 (s), 1346 (s), 1493 (s), 1678 (s), 2913(br), 1118.2 (s), 3123 – 3240 (br) and 3337 (br).

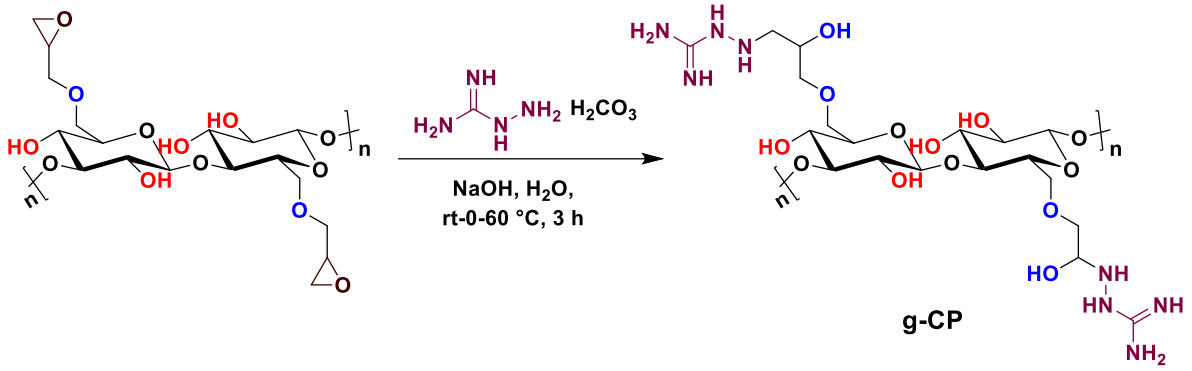

Scheme S2. Synthesis of guanidine functionalized cellulose polymer (g-CP).

2.3. Synthesis of Zn-gCP — The gCP (0.2 g) was added into a stirring solution of $ZnCl_2.6H_2O$ (0.05 g) in water, and the reaction mixture was stirred at 100 °C for 12 h. Then, the reaction mixture was centrifuged at 6000 rpm for 10 min, followed by filtration, and the precipitate was repeatedly washed off with deionized water. Finally, the solid part was oven-dried overnight at 70 °C to obtain Zn(II)-loaded aminated polymer (Scheme S3). **Characterization of the compound:** solid-state FT-IR (cm^{-1}) = 442 (br), 1017 (s), 1111 (s), 1346 (s), 1493 (s), 1678 (s), 2913 (br), 1118.2 (s), 3123 – 3240 (br) and 3337 (br).

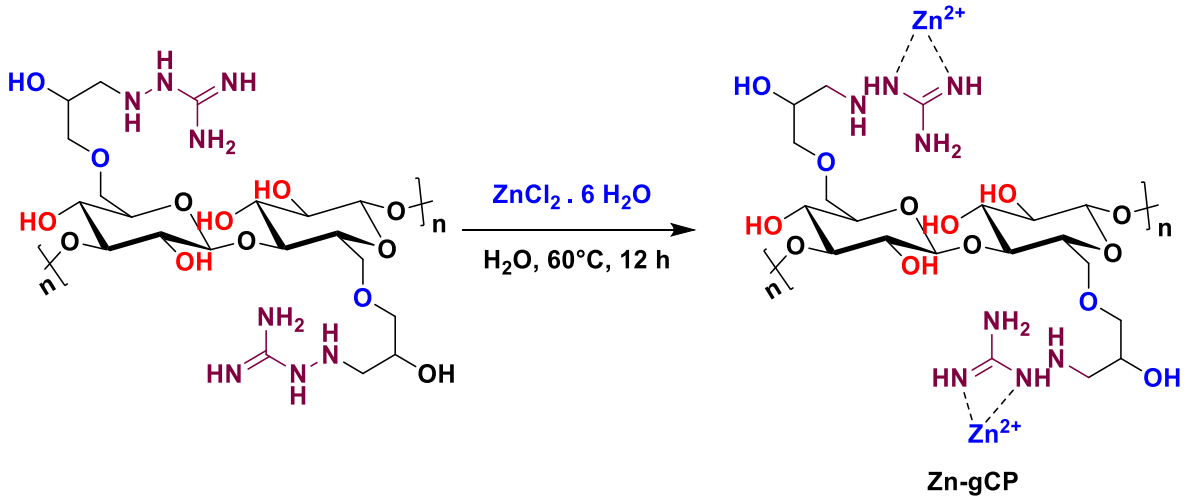

Scheme S3. Synthesis of Zn-complex-guanidine functionalised cellulose (Zn-gCP).

2.4. Fourier-Transform Infrared spectroscopy (FT-IR) —

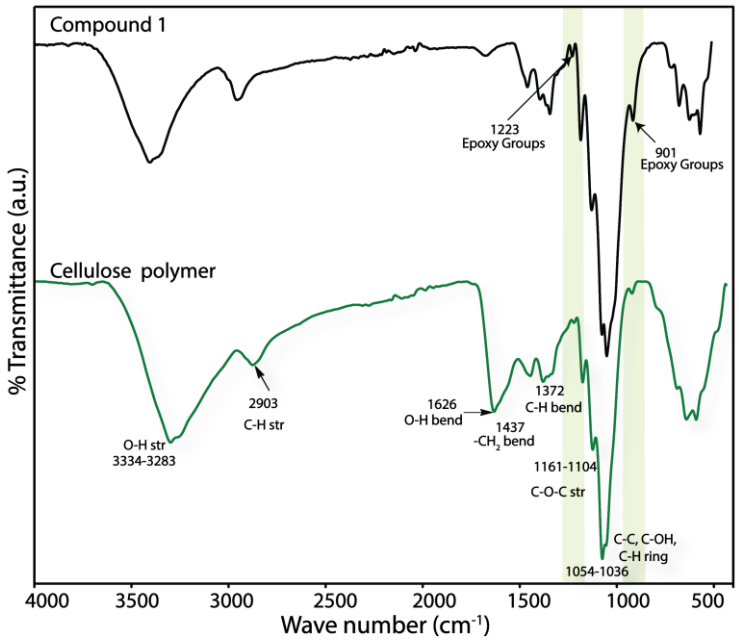

Fig. S1. FT-IR of cellulose and compound **1**.

2.5. X-ray photoelectron spectroscopy (XPS) — For the XPS analysis, the samples were prepared using the drop-casting dispersion method. The polymer (<0.5 mg) was dispersed in an aqueous solution (~1 mL) and deposited onto a silicon substrate, followed by incubation at room temperature to dry the sample before analysis.

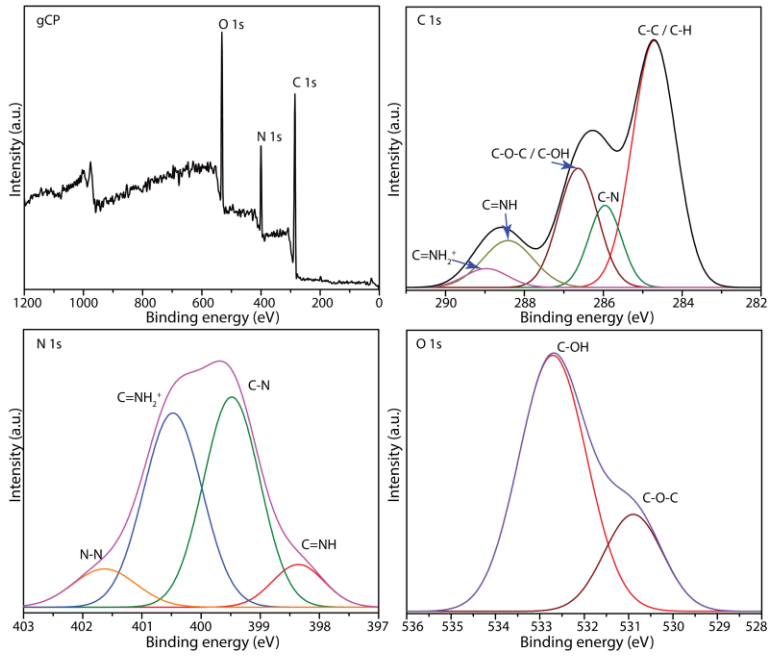

Fig. S2. The XPS analysis of gCP polymers and XPS data profile: wide scan of gCP polymers, the deconvoluted peak of C 1s, N 1s, and O 1s.

2.6. Field Emission Scanning Electron Microscopy (FESEM) and FESEM - Energy Dispersive X-Ray Spectroscopy (FESEM-EDX) analysis— For FESEM and FESEM-EDX analysis, the samples were prepared using the drop-casting dispersion method. The polymer (< 0.5 mg) was dispersed in an aqueous solution (~1 mL) and deposited onto a silicon substrate, followed by incubation at room temperature to dry the sample before analysis.

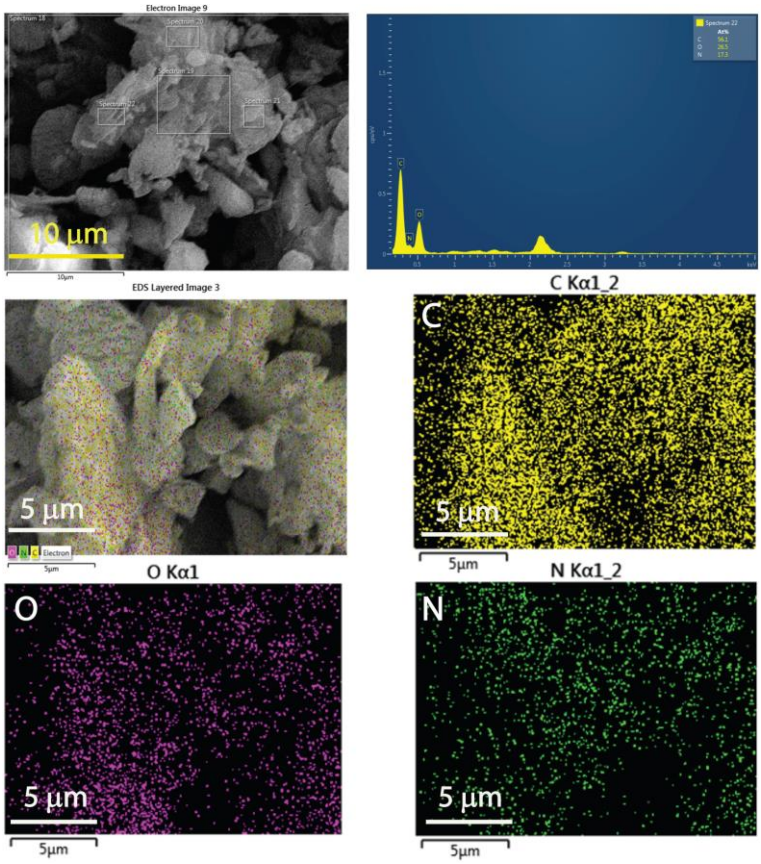

Fig. S3. FESEM-EDX elemental mapping analysis of gCP polymer.

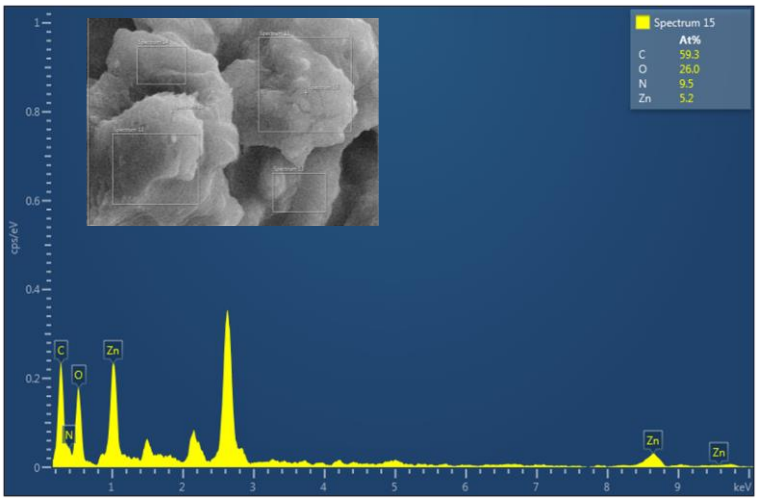

Fig. S4. FESEM-EDX analysis of Zn-gCP polymer.

2.7. Thermogravimetric analysis (TGA) — TGA were conducted by heating the samples (10 mg) from 20 °C to 900 °C, and the rate of heating was 10 °C min^{-1}.

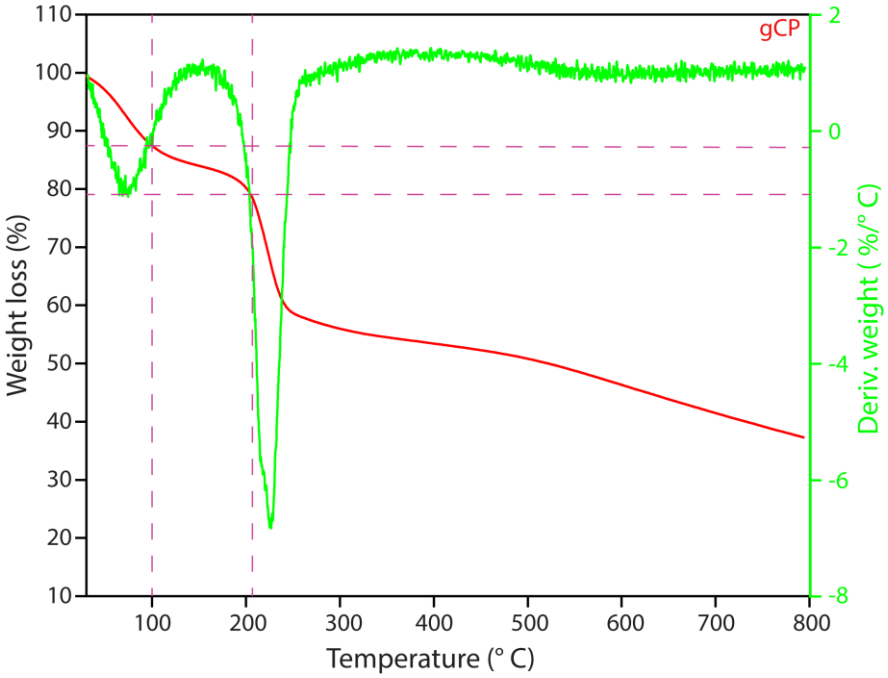

Fig. S5. TGA-DTG plot of gCP polymer.

2.8. Dynamic Light Scattering (DLS) study — In order to perform DLS measurements, ≤ 0.5 mg of the polymers were mixed with 1 mL of Milli-Q water and then exposed to sonication for a period of 10 min. Subsequently, the hydrodynamic diameter was assessed at different time intervals (0 h, 12 h, 24 h, 36 h, and 72 h) at a temperature of 25°C.

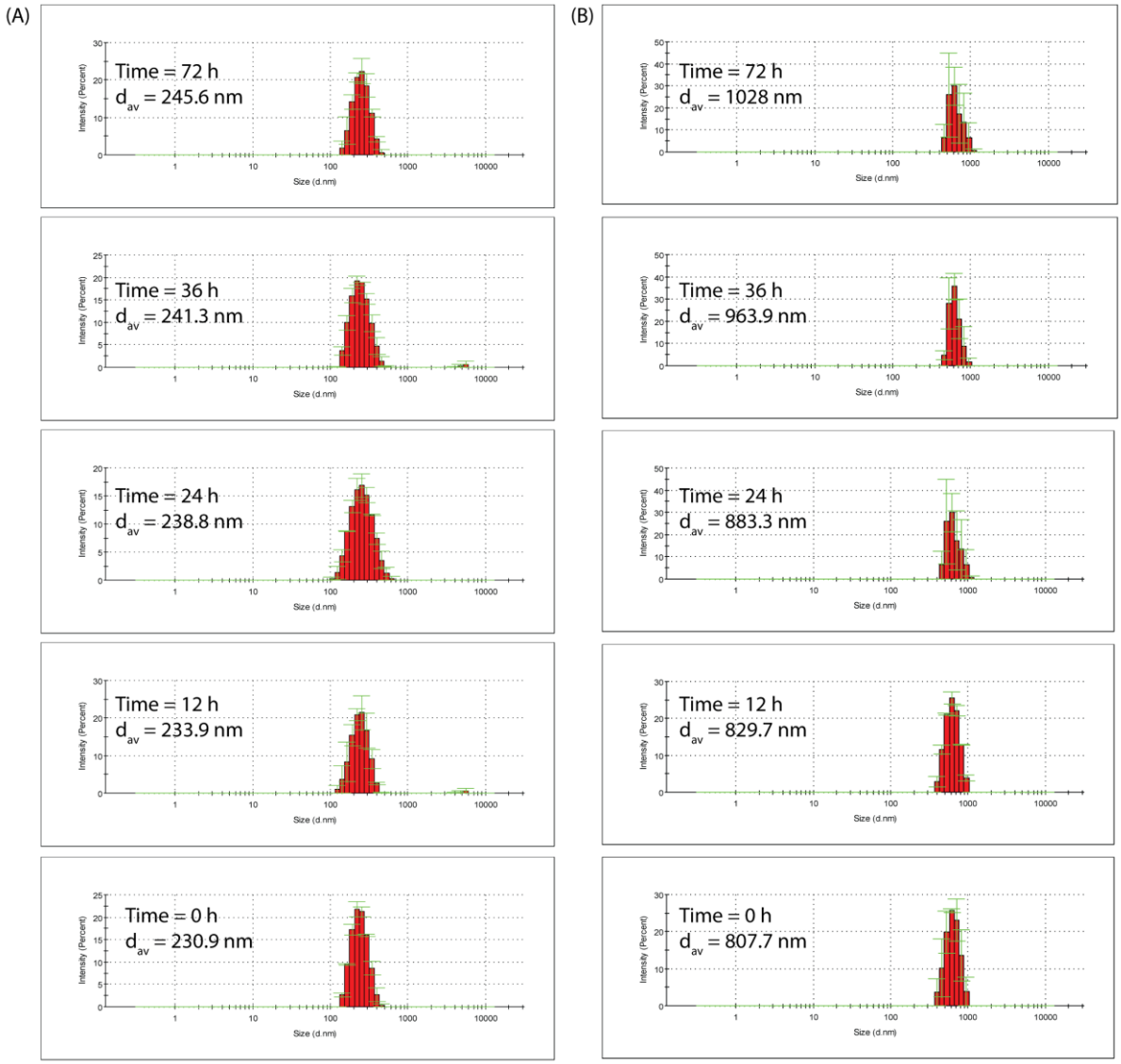

Fig. S6. DLS measurements of unmodified cellulose (A) and Zn-gCP (B) in water at different time intervals.

2.9. Zeta potential measurements — The zeta potential of all the samples was measured at 25 °C across a range of pH values (2, 4, 5, 6, 7, 8, and 10). In this experiment, ≤ 0.5 mg of the polymers were mixed with 1 mL of Milli-Q water and then exposed to sonication for a period of 10 min before analysis. The pH of the solutions was adjusted by using 0.1 M HCl and 0.1 M NaOH solutions.

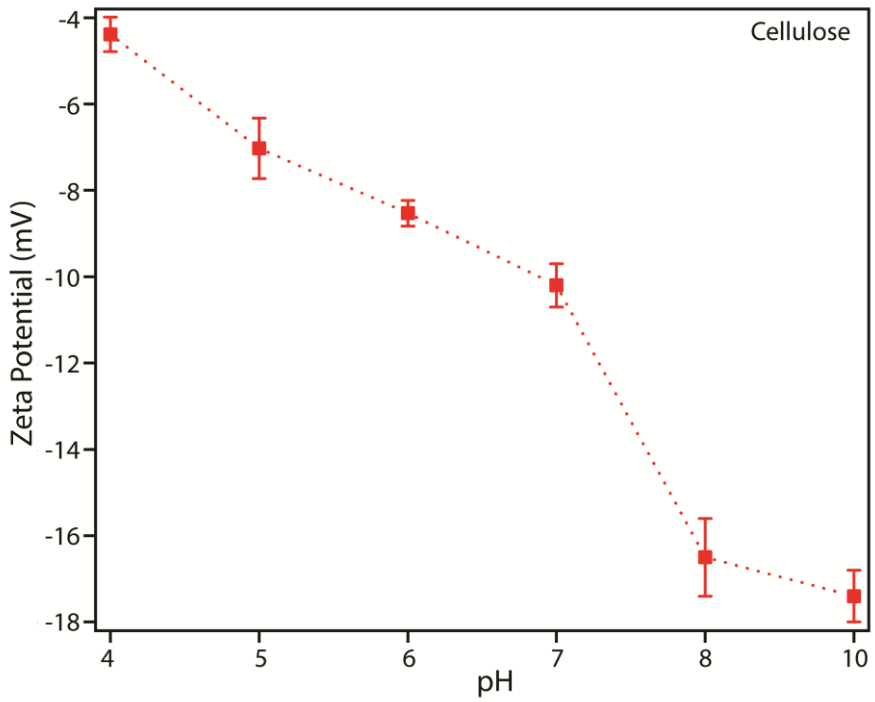

Fig. S7. Zeta potential of the cellulose at different pH.

2.10. Chemical stability for gCP and Zn-gCP polymers — To assess the chemical stability of gCP and Zn-gCP polymers, 5 mg of each polymer was separately treated with 5 mL of common organic solvents, including acetonitrile (ACN), ethyl acetate (EtOAc), methanol (MeOH), and tetrahydrofuran (THF) for 7 days at room temperature. The polymers were then separated from the solvents by centrifugation at 6000 rpm for 10 min, followed by filtration, and dried in an oven at 70 °C for 6 h, followed by FT-IR analysis to examine their chemical stability. Additionally, to evaluate stability under acidic and basic conditions, 5 mg of each polymer was treated with 5 mL of HCl (0.5 N) and NaOH (0.5 N) for 7 days at room temperature. After this treatment, the polymers were separated by centrifugation (6000 rpm for 10 min) and dried under the same conditions, and their chemical stability was examined by FT-IR and TGA analysis.

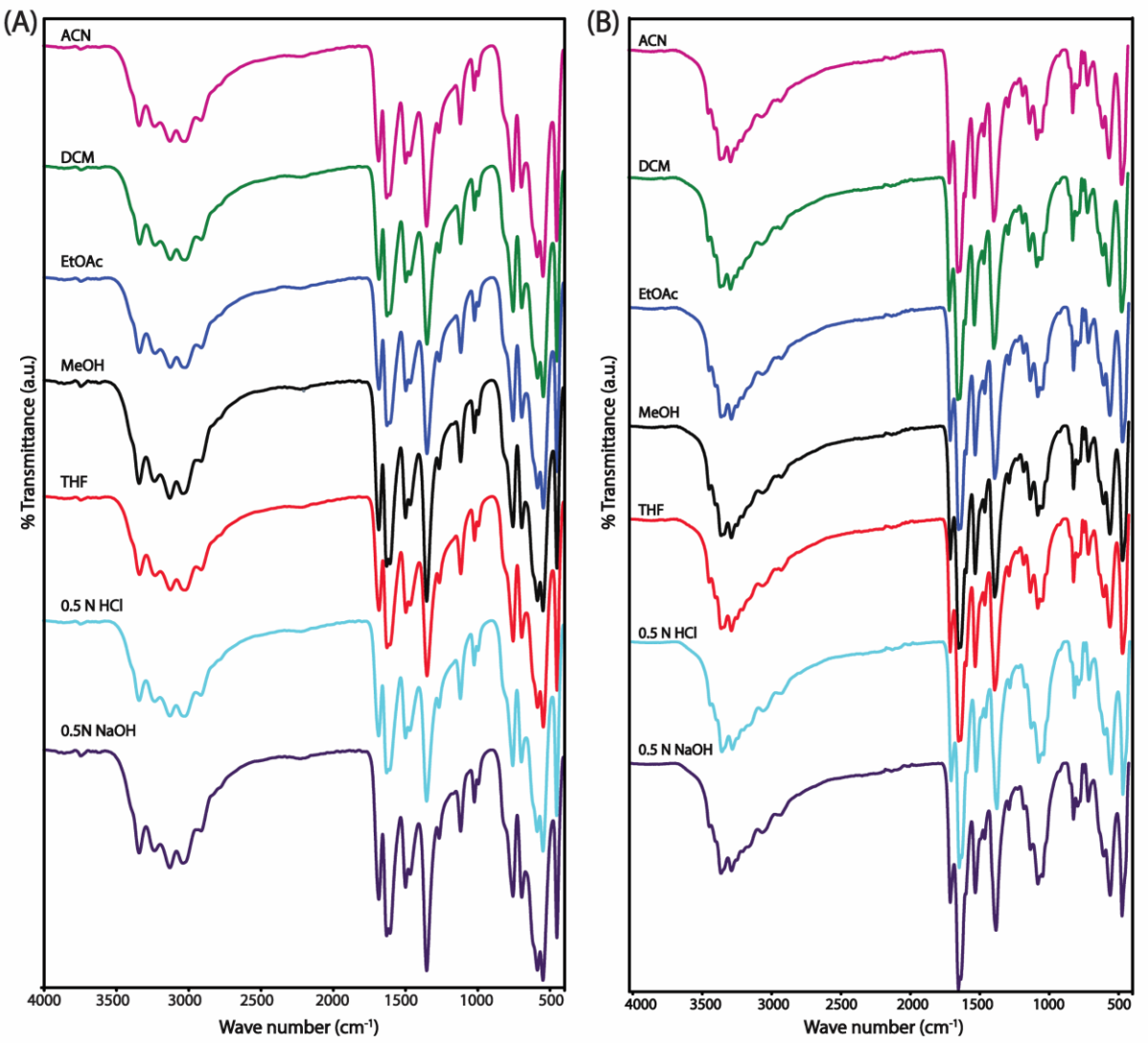

Fig. S8. FT-IR spectra of gCP (A) and Zn-gCP (B) after the treatment (for 7 days) with ACN, DCM, EtOAc, MeOH, THF, DMF, HCl (0.5N), and NaOH (0.5N) solution.

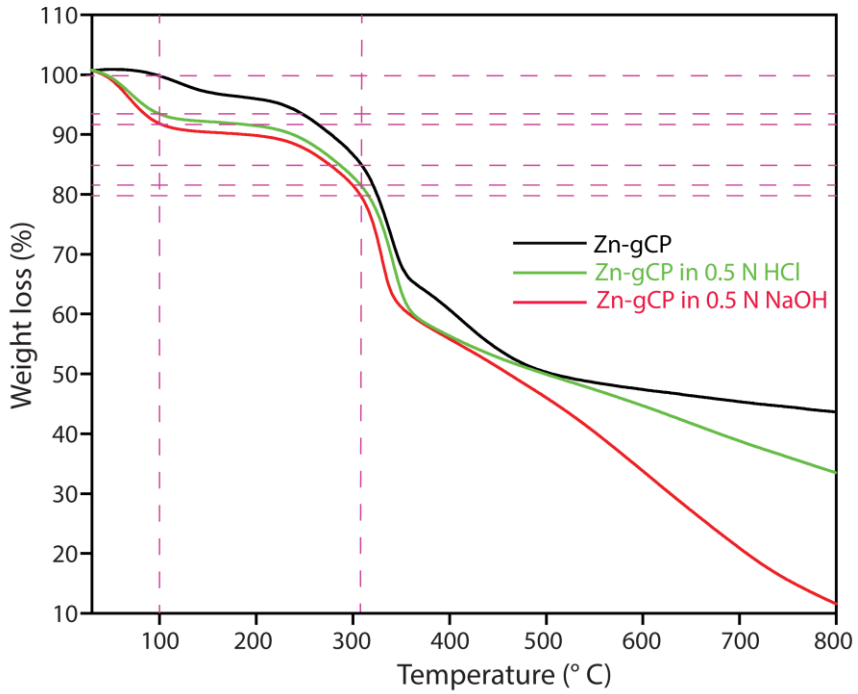

Fig. S9. TGA plot of Zn-gCP polymer, Zn-gCP after treatment with 0.5 N HCl, and 0.5 N NaOH.

NOTE: After treatment of the Zn-gCP polymer with 0.5 N HCl for 7 days, there is a potential for the protonation of the guanidine -NH groups, which may weaken the Zn(II) coordination sites. Conversely, when the polymer is treated with 0.5 N NaOH for 7 days, the high concentration of OH^- ions could lead to the leaching of some Zn(II) ions from the polymer, forming complexes with OH^- ions. Hence, the weight loss against temperature differs in each case, but the maximum weight loss is observed at approximately the same temperature (~ 350 °C).

2.11. Tyndall effect — In order to examine the Tyndall effect, a small quantity (<1mg) of Zn-gCP (B) and gCP (D) was individually mixed with deionized water (5 mL) and subjected to 5 min of sonication. Both the polymer solutions were then exposed to laser light, with a reference solution of normal deionized water serving as a control in each case (A for Zn-gCP and C for gCP)

3. Adsorption study:

3.1. Calculation of % ion adsorption — To calculate the relative percentage of phosphate adsorption, the following equation has been used for calculation:

Percentage of adsorption,

$$Qad(\%) = \frac{(Co-Ce)}{Co} * 100\% \ldots \text{Eq. (1)}$$

Where Q_{ad} is the relative percentage adsorption, C_0 and Ce is the concentration of anions in ppm (mg/L) before and after treatment of polymers, respectively.

3.2. Calculation for adsorption capacity — The adsorption capacity of Zn-gCP polymer was calculated by the following Eq. (2).

$$Q_e = \frac{(C_0-C_b)}{m} V\ n\ M \ldots \text{Eq. (2)}$$

Where, Q_e = equilibrium adsorption capacity (mg g^{-1}), Co = initial concentration (in ppm), C_e = equilibrium concentration (in ppm), V = volume of solution, m = amount of adsorbent (mg), n = dilution factor, and M = molecular weight of ion.

3.3. Adsorption isotherm experiment — To explore the adsorption patterns, Langmuir isotherm (Eq. (3)), and Freundlich isotherm models (Eq. (4)) were used to fit the adsorption data.

$$Q_e = \frac{Q_m K_l C_e}{1 + K_l C_e} \ldots \text{Eq. (3)}$$

$$Q_e = K_f C_e^{1/n} \ldots \text{Eq. (4)}$$

Where Ce is the equilibrium phosphate concentration (ppm), Q_e is the corresponding adsorption capacity (mg g^{-1}). The K_l is the Langmuir constant, and Q_m (mg g^{-1}) is the max adsorption capacity for the Langmuir model. The K_f and n are the Freundlich constants. For Freundlich adsorption isotherm, the K_f is associated with the adsorption capacity of the polymer. Whereas 1/n describes the extent of adsorption (favourable $1/n < 1$ or unfavourable $1/n > 2$).

3.4. Adsorption kinetics equations — To explore the sorption mechanism, the time-dependent adsorption data were fitted with both the linear (Eq. (5)) and non-linear (Eq. (6)) pseudo-first-order kinetics models, as well as the linear (Eq. (7)) and non-linear (Eq. (8)) pseudo-second-order kinetics models, as described below:

$$\ln(Q_e - Q_t) = lnQ_e - k_1 t \ \ldots \text{Eq. (5)}$$

$$Q_t = Q_e(1 - e^{-k_1 t}) \ldots \text{Eq. (6)}$$

$$\frac{t}{Q_t} = \frac{1}{Q_e^2 k_2} + \frac{t}{Q_e} \ldots \text{Eq. (7)}$$

$$Q_t = \frac{k_2 {Q_e}^2 t}{1+k_2 Q_e t} \ldots \text{Eq. (8)}$$

Where Q_t and Q_e (mg g^{-1}) are the adsorption capacities of phosphate ions at time t and at equilibrium, respectively. The k_1 and k_2 (g mg min^{-1}) are the adsorption rate constants of the pseudo-first-order and pseudo-second-order equations, respectively.

4. Anion Selectivity Study:

To determine anion selectivity by gCP and Zn-gCP polymer, a stock solution was prepared containing various anions from sodium salts (such as F^-, Cl^-, Br^-, NO_3^-, SO_4^{2-}, and phosphate) in Milli-Q water at ~25 ppm concentration for each ion. 5 mg of each polymer (gCP and Zn-gCP) were individually mixed with 5 mL of the stock solution and agitated for 12 h after that, the polymers were separated from the stoke solution by centrifugation at 6000 rpm for 10 min, followed by filtration. The IC was used to assess the concentration of anions before and after treatment of the polymer (gCP and Zn-gCP).

4.1. The affinity of the gCP and Zn-gCP towards chromate and dichromate ions — 5 mg of the gCP and Zn-gCP polymers were separately treated with 5 mL of ~25 ppm stock solutions of the sodium salts of chromate and dichromate. The mixtures were agitated for 6 hours at room temperature. Following that, the polymers were separated by centrifugation at 6000 rpm for 10 minutes, followed by filtration. The concentrations of chromate and dichromate ions before and after treatment were quantified using UV-Vis spectroscopy at 373 nm and 260 nm, respectively, using. The results revealed that the gCP and Zn-gCP polymers exhibited >20% and >30% removal efficacy of chromate, respectively, from the water. Similarly, the gCP and Zn-gCP polymers also manifest low removal efficacy, >17% and >25% of dichromate, respectively, under the same conditions.

4.2. The affinity of the gCP and Zn-gCP towards arsenate ions — 5 mg sample of the gCP and Zn-gCP polymers was separately treated with 5 mL of ~25 ppm stock solution of sodium arsenate and agitated for 6 hours at room temperature. The polymers were then separated from the reaction mixture by centrifugation at 6000 rpm for 10 minutes, followed by filtration. The concentration of arsenate in the solution before and after treatment was determined using Atomic Absorption Spectroscopy after diluting all samples 500-fold. The results indicated that the gCP and Zn-gCP polymers exhibited >43% and >59% removal efficacy of arsenate, respectively, from the stock solution.

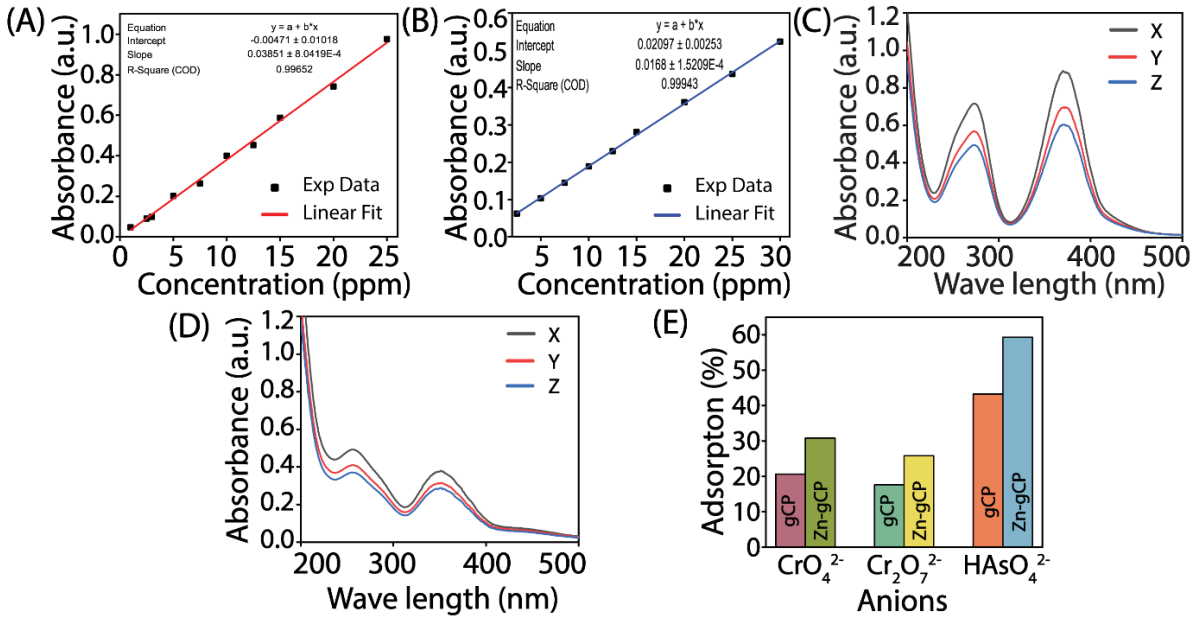

Fig. S10. Standard calibration plot of the chromate (A), and dichromate (B) at different concentrations. UV-Vis spectra of stoke solution, after treatment with gCP and Zn-gCP polymer of chromate (C) and dichromate (D). Adsorption efficacy of gCP and Zn-gCP for chromate, dichromate and arsenate (E). (Note: X, Y, and Z are the absorbance of stoke solution after treatment with gCP and Zn-gCP polymer, respectively).

5. Phosphate Adsorption Experiments:

5.1. Influence of pH on phosphate capture — To check the pH-dependency of phosphate adsorption by Zn-gCPs, seven different sets of pH values were selected for the adsorption experiments: pH 2, 4, 5, 6, 7, 8, and 10. The pH of the solutions was adjusted by HCl (0.1 M) and NaOH (0.1 M). The Zn-gCPs (5 mg) and 1000 ppm phosphate solutions (5 mL, pH = 2, 4, 5, 6, 7, 8, and 10) were mixed together and stirred at room temperature for 6 h. After that, samples were collected, and the polymers were separated by centrifugation at 6000 rpm for 10 min followed by filtration. The filtered supernatant was diluted to maintain the concentration of phosphate to 25 ppm, and an IC-based assay was performed in these solutions to measure the residual phosphate ions.

5.2. Adsorption Isotherms — Different concentrations of phosphate ranging from 25 to 1000 ppm in 5 mL water were treated with a fixed quantity of (5 mg) gCP and Zn-gCP, and sonicated for 10 min to homogenize the polymer. Then, the samples were incubated at shaking conditions for 6 h at room temperature. After that, the samples were centrifuged at 6000 rpm

for 10 min and filtered to separate the phosphate-adsorbed Zn-gCP and unbound phosphate in the supernatant, which was further diluted up to 25 ppm and measured in IC.

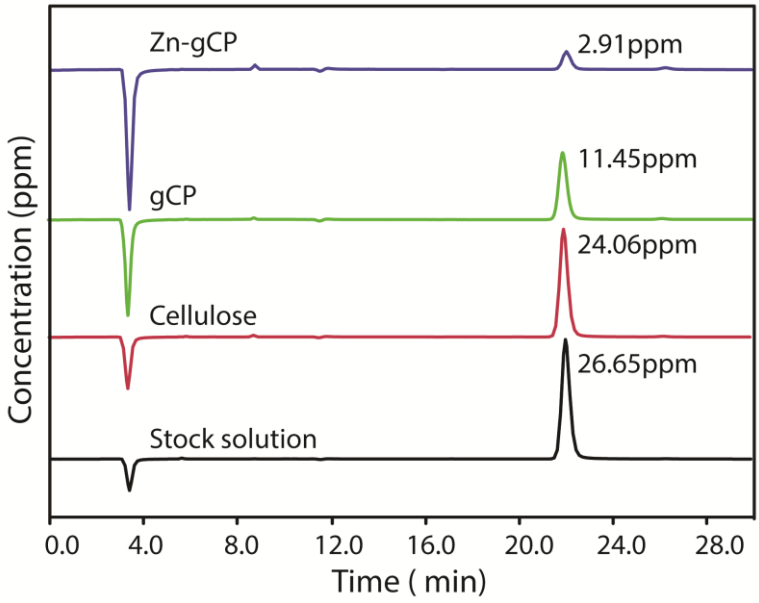

Fig. S11. Phosphate adsorption efficacy of different polymers including cellulose, gCP and Zn-gCP polymer.

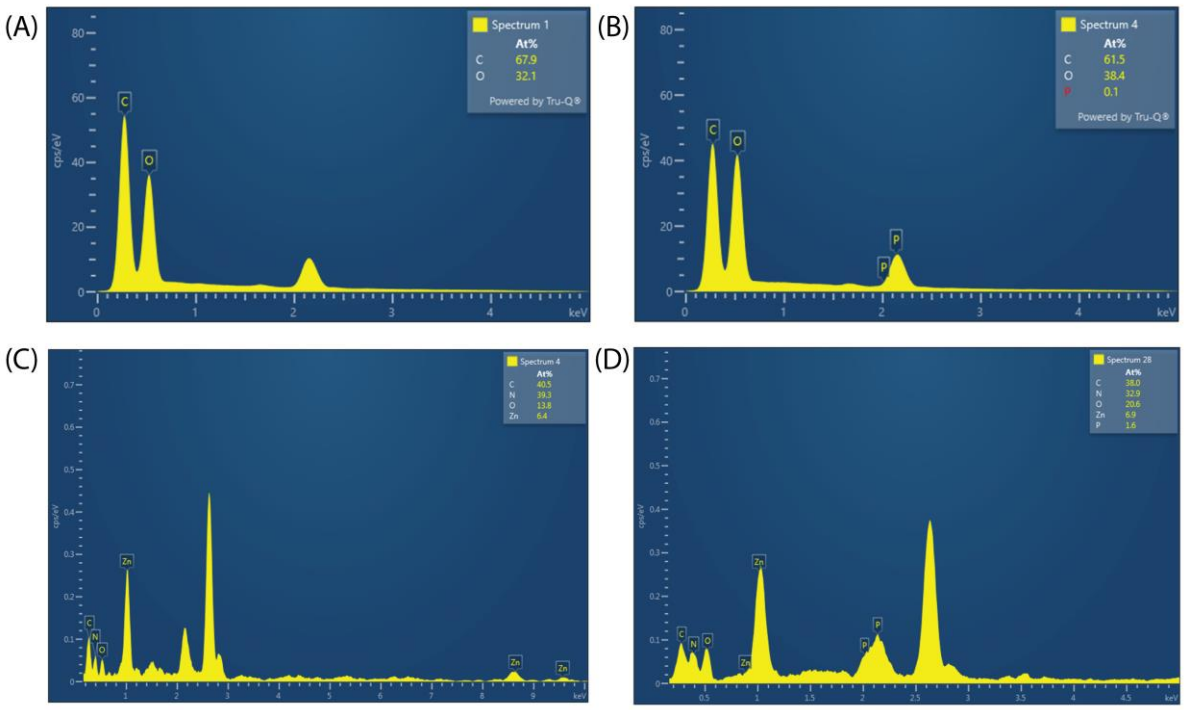

Fig. S12. FESEM-EDX Elemental analysis of Unmodified cellulose before phosphate treatment (A), after phosphate treatment (B), Zn-gCP polymer before phosphate treatment (C), and after phosphate treatment (D).

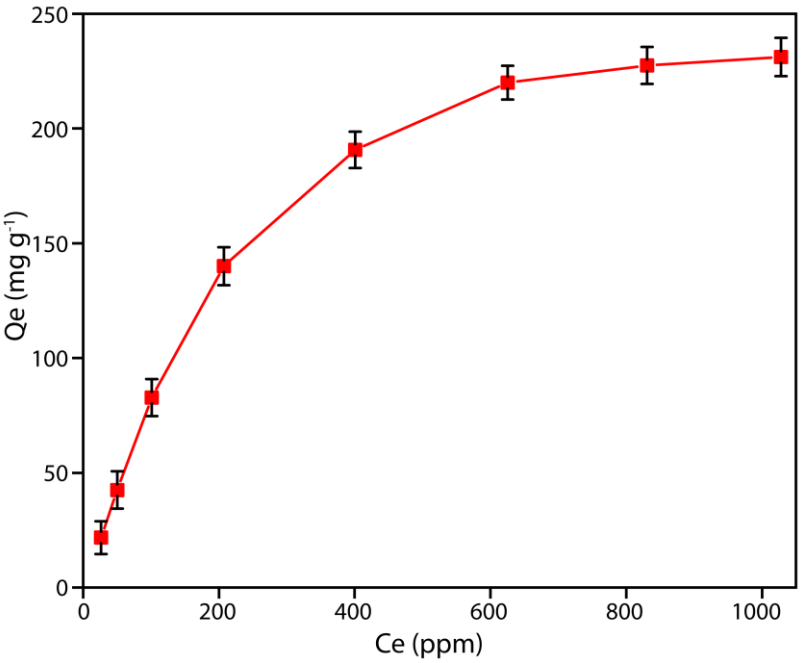

Fig. S13. Phosphate adsorption isotherm of Zn-gCP (5 mg) at pH 7.0 under room temperature.

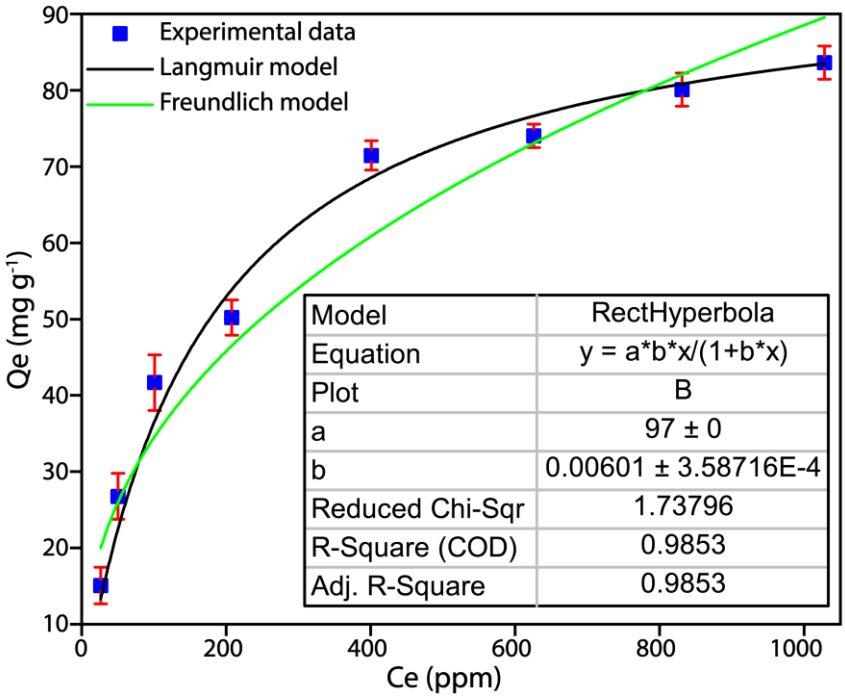

Fig. S14. Phosphate adsorption isotherm of gCP (5 mg) at pH 7.0 under room temperature.

5.3. Kinetics study — The phosphate adsorption kinetics onto gCP and Zn-gCP polymer over time were investigated by incubating the 5mg of the adsorbent (gCP and Zn-gCP) into 1000 ppm concentration of phosphate salt in Milli-Q water at pH ~7. At different time intervals (2, 4, 6, 8, 10, 20, 30, 40, and 60 min), samples were collected, and the polymers were separated

by centrifugation at 6000 rpm for 10 min followed by filtration. The filtered supernatant was diluted up to 40 times to achieve a phosphate concentration of 25 ppm, which was then quantified using IC.

Additionally, a kinetics study was conducted with different amounts of Zn-gCP polymer (3 mg, 5 mg, 7 mg, and 10 mg) under the same conditions. The polymer samples were subjected to incubation in a 1000 ppm phosphate salt solution in Milli-Q water at pH ~7, followed by sample collection at the aforementioned time intervals, and the polymers were separated by centrifugation at 6000 rpm for 10 min, followed by filtration. The filtered supernatant was diluted up to 40 times to achieve a phosphate concentration of 25 ppm, which was then quantified using IC.

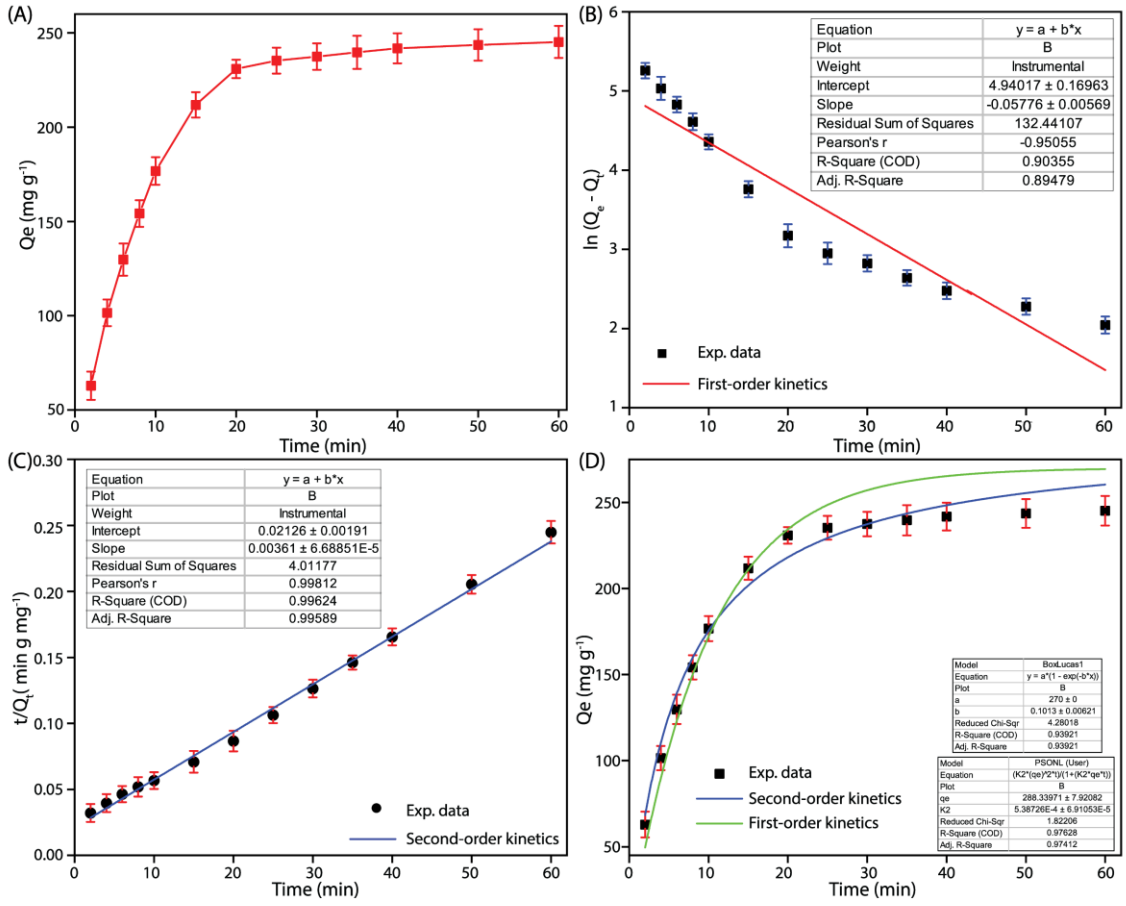

Fig. S15. Time-dependent adsorption isotherm of phosphate by Zn-gCP (5mg) at pH 7 under room temperature(A), time-dependent adsorption efficiency of Zn-gCP (5 mg) fitted with the linear first order(B), linear second order (C), and non-linear first and second order kinetics model (D).

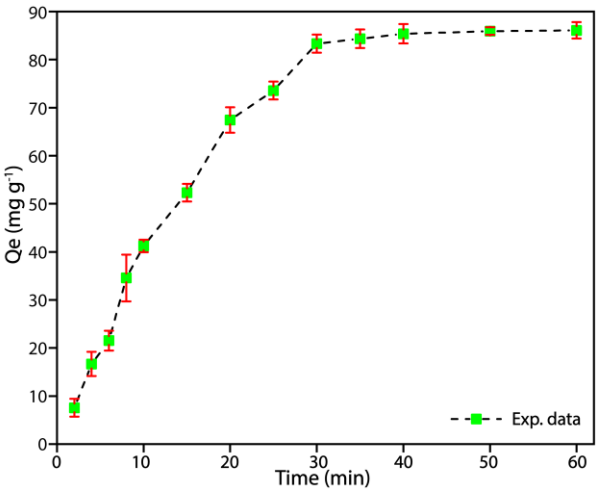

Fig. S16. Time-dependent adsorption isotherm of phosphate by gCP (5mg) at pH 7 under room temperature.

5.4. Effect of counter anions on phosphate adsorption — To assess the impact of competing anions on phosphate adsorption, stock solutions of several sodium salts (F^-, Cl^-, Br^-, NO_3^-, SO_4^{2-}, and phosphate) were prepared by dissolving them in Milli-Q water at a 1:2 concentration ratio (phosphate: other anions). The Zn-gCP polymer (5 mg) was mixed with 5 mL of the salt solution and agitated for 6 h after that, the polymers were separated from the stoke solution by centrifugation at 6000 rpm for 10 min, followed by filtration. The ability of the Zn-gCP polymer to adsorb phosphate ions in the presence of the other competing anions was assessed using IC.

Table S1: Phosphate removal efficacy of Zn-gCP in the presence of other anions.

Solutions	Initial concentration of Phosphate in presence of other anions (ppm)	Concentration of Phosphate in presence of other counter anions after treatment of with Zn-gCP (ppm)	% of removal of Phosphate in presence of other counter anions after the treatment with Zn-gCP
Only Phosphate	25.369 ± 0.045	0.490 ± 0.245	98.066 ± 0.484
Phosphate + F^-	26.480 ± 0.018	3.261 ± 0.325	87.685 ± 0.618
Phosphate + Cl^-	25.095 ± 0.033	2.121 ± 0.503	91.548 ± 1.007
Phosphate + Br^-	25.172 ± 0.051	1.488 ± 0.402	94.086 ± 0.804
Phosphate + NO_3^-	25.155 ± 0.032	3.678 ± 0.494	85.378 ± 0.992

Phosphate + SO_4^{2-}	26.005 ± 0.016	4.449 ± 0.658	82.890 ± 1.260
Phosphate + F^- + Cl^- + Br^- + NO_3^-+ SO_4^{2-}	25.400 ± 0.014	5.460 ± 0.811	78.502 ± 1.602

5.5. Low-concentration of phosphate capture study — To performed the experiment, 5 mg of the Zn-gCP polymer was treated with the phosphate solutions of volumes 50 mL at an initial concentration of 5 ppm and agitated for 6 hours. Following this, the polymer was separated from the solution via centrifugation at 6000 rpm for 10 min followed by filtration, and the concentrations of phosphate ion in the solution before and after treatment with the Zn-gCP polymer were measured using IC.

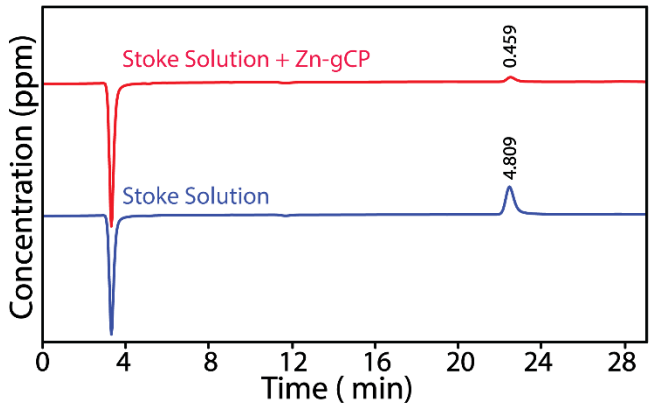

Fig. S17. Low concentration phosphate ion adsorption study by Zn-gCP polymer.

5.6. Phosphate removal applicability with the real phosphate contaminated wastewater — To evaluate the efficacy of Zn-gCP polymers in removing phosphate ions from real-world eutrophic water, two samples were collected from two different food manufacturing industries located in North Guwahati, Assam, India. The pH, ion concentrations, phosphate, and other coexisting species are all listed in Table S2. The Zn-gCP polymers (5 mg) were treated with 5 mL of each sample, and the mixture was constantly stirred for 6 h. IC was used to determine the anion concentration after centrifuging (6000 rpm for 10 min) and filtering the solution to remove the polymer. The study demonstrated that the Zn-gCP polymers successfully reduced phosphate ion concentration to below the WHO-recommended level for phosphate discharge, even in the presence of other coexisting anions. These results indicate that the synthesized Zn-gCP polymers could function as an effective adsorbent for removing phosphate from

wastewater. The experiments were repeated three times, and the error bars in the figures represent the standard deviations of these three experiments.

Table S2. IC analysis demonstrating the concentrations of different competitive anions present before and after the treatment of Zn-gCP of samples A and B.

Sample	Existing anions (concentration in ppm)						pH
	F^-	Cl^-	Br^-	NO_3^-	Phosphate	SO_4^{2-}	
Sample A	1.161 ± 0.071	13.028 ± 0.031	0.307 ± 0.047	3.954 ± 0.05	8.012 ± 0.117	11.077 ± 0.077	5.6
After Zn-gCP treatment of sample A (A′)	1.002 ± 0.051	11.105 ± 0.022	0.247 ± 0.041	3.067 ± 0.036	0.419 ± 0.053	8.719 ± 0.057	
Sample B	1.61 ± 0.039	14.69 ± 0.061	0.271 ± 0.05	3.041 ± 0.029	6.971 ± 0.103	10.22 ± 0.063	6.1
After Zn-gCP treatment of sample B (B′)	0.297 ± .02	12.091 ± .04	0.190 ± 0.032	2.876 ± 0.022	0.398 ± 0.069	7.374 ± 0.053	

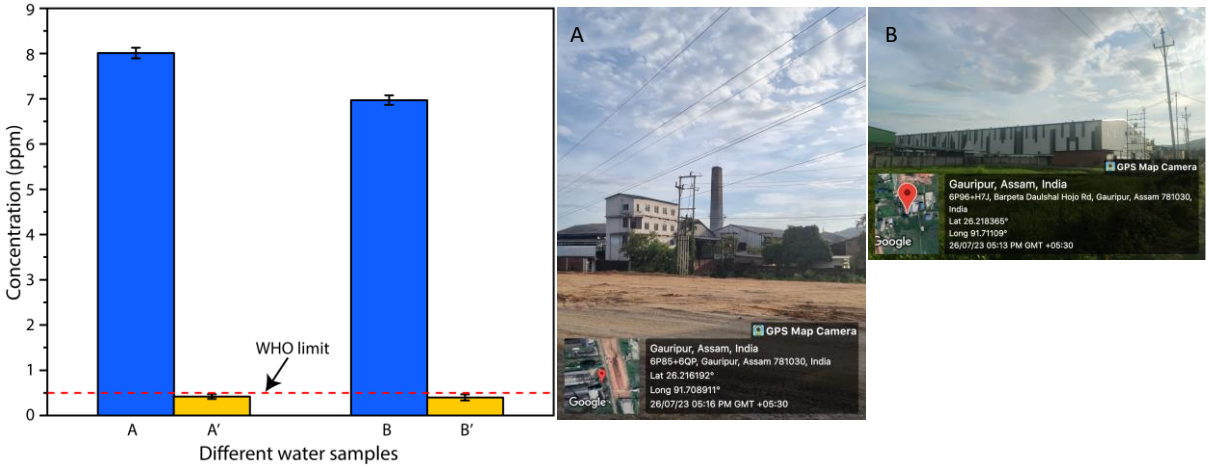

Fig. S18. Phosphate adsorption capacity of the Zn-gCPs from the real phosphate-contaminated wastewater.

5.7. Phosphate recovery and regeneration of the Zn-gCP— The adsorption percentage for each cycle was calculated using Equation 9, while the desorption efficiency for each cycle was calculated using Equation 10. The adsorption percentage for each cycle was calculated by taking the equilibrium adsorption capacity (Q_o) of the first cycle as 100%, and the adsorption percentage of subsequent cycles was expressed relative to this reference value. Conversely, the desorption percentage for each cycle was calculated considering the corresponding equilibrium adsorption capacity (Q_e) for that cycle as 100%).

$$Qad(\%) = \frac{Qe}{Qo} * 100\% \ldots \text{Eq. (9)}$$

$$Qde(\%) = \frac{Qi}{Qe} * 100\% \ldots \text{Eq. (10)}$$

Where Q_{ad} (%) and Q_{de} (%) are the relative percentages of adsorption and desorption, respectively. Q_o is the equilibrium phosphate adsorption capacity in the first adsorption cycle. The Q_e is the equilibrium phosphate adsorption capacity in each adsorption cycle. The Q_i is the equilibrium phosphate desorption capacity in each desorption cycle.

After undergoing the 1st, 5th, and 10th desorption cycles, the concentration of Zn(II) ions in the solution was quantified using Inductively Coupled Plasma Mass Spectrometry (ICP-MS). This analysis was conducted to evaluate the leaching of Zn(II) ions from the polymer network over multiple desorption cycles, providing insights into the stability and retention of Zn(II) within the polymer matrix.

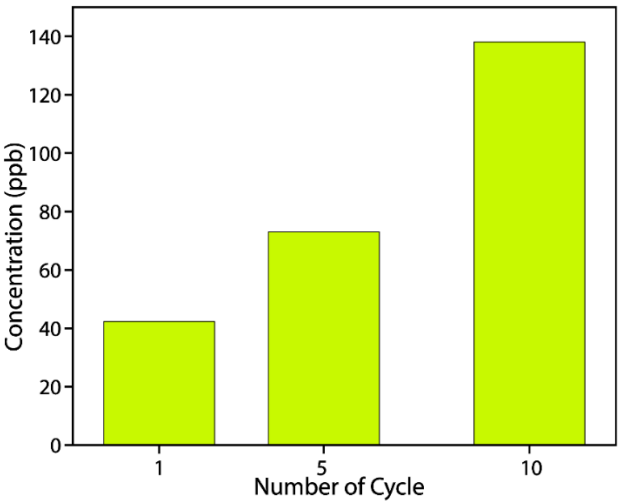

Fig. S19. Concentration of Zn(II) in the solution after undergoing 1st , 5th and 10th cycle of desorption.

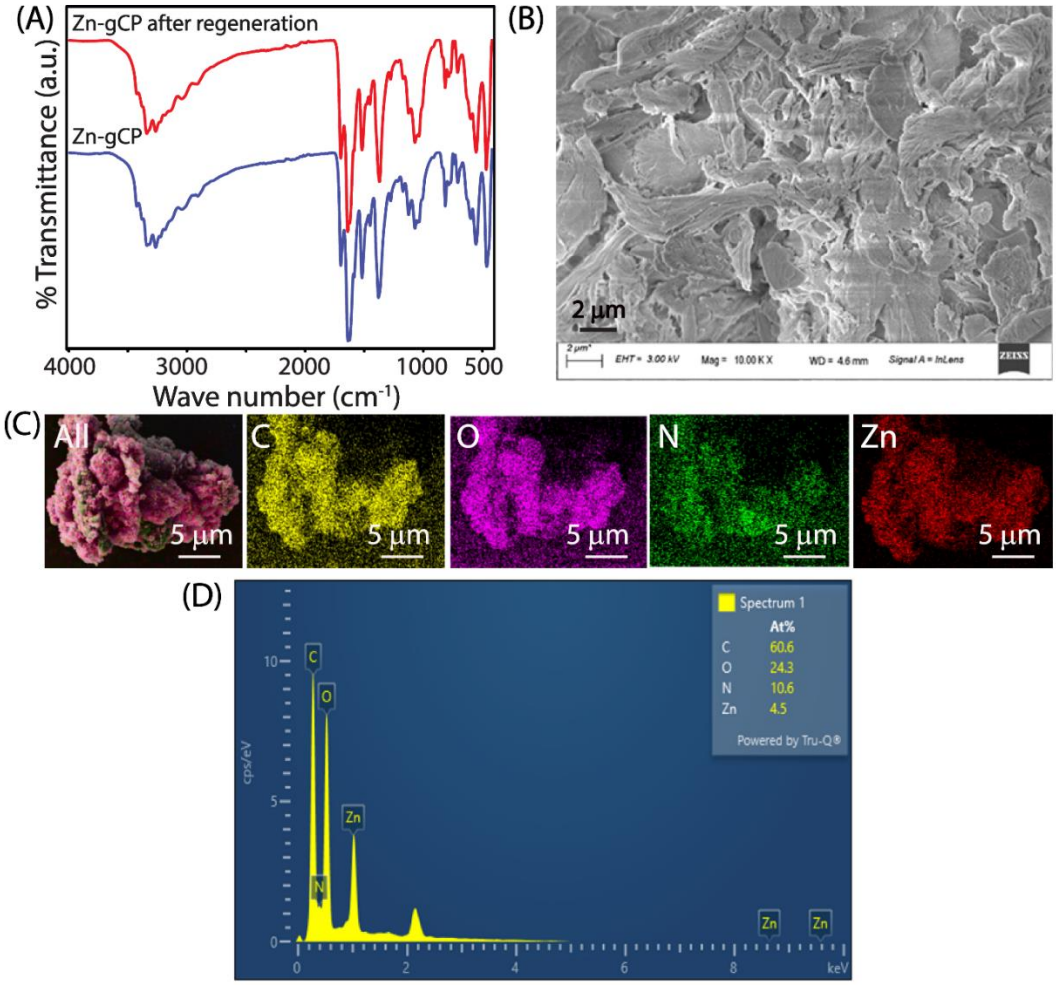

Fig. S20. FTIR spectra (A), FESEM image (B), FESEM-Elemental mapping (C) and FESEM-EDX analysis (D) of Zn-gCP after undergoing ten cycles of regeneration.

5.8. Phosphate desorption kinetics — To study the desorption of phosphate from the Zn-gCP polymer, first the phosphate-loaded polymers (5 mg) were mixed with 5 mL of 0.5 N NaOH (pH ~13), and the solution was continuously stirred by an orbital shaker incubator (LabTech) at 180 rpm and 25 ºC. At different time intervals (2, 4, 6, 8, 10, 20, 30, 40, and 60 min), samples were collected, and the polymers were separated by centrifugation at 6000 rpm for 10 min, followed by filtration. The filtered supernatant was diluted 10 times to maintain the concentration of phosphate to 25 ppm and quantified by IC.

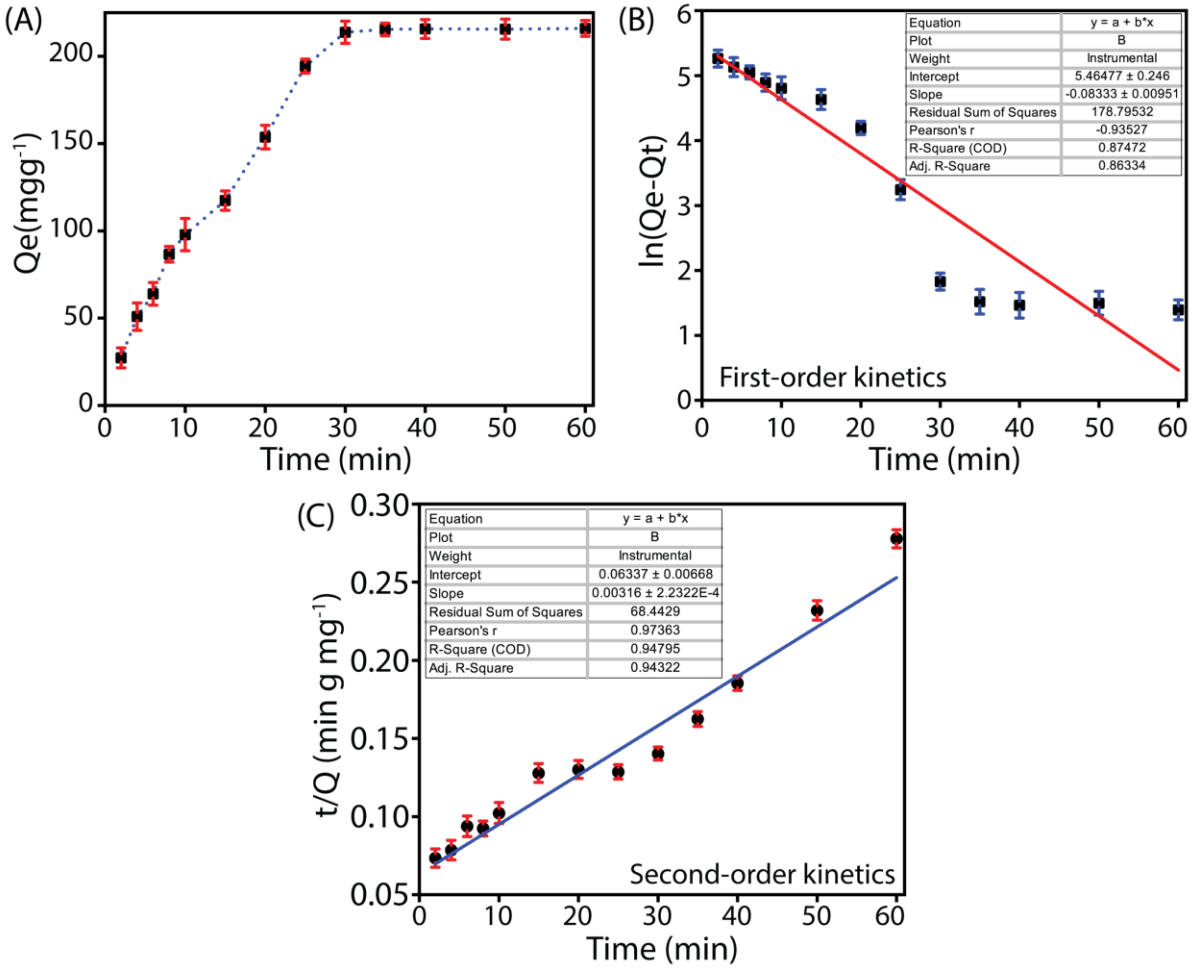

Fig. S21. Time-dependent desorption isotherm of phosphate by Zn-gCP (5mg) at pH 7 under room temperature(A), time-dependent desorption efficiency of Zn-gCP fitted with the first order(B) and second order kinetics(C) models.

5.9. Phosphate desorption kinetics study with different amounts of phosphate loaded Zn-gCP polymer— Phosphate desorption tendency from Zn-gCP as per time was analyzed by incubating the different amounts of the phosphate loaded Zn-gCP polymer (3 mg, 5 mg, 7 mg, 10 mg) into 5 mL of 0.5 N NaOH (pH 11.5). At different time intervals (2, 4, 6, 8, 10, 20, 30,

40, and 60 min), samples were collected, and the polymers were separated by centrifugation followed by filtration. The filtered supernatant was diluted to maintain the phosphate concentration to 25 ppm and quantified by IC.

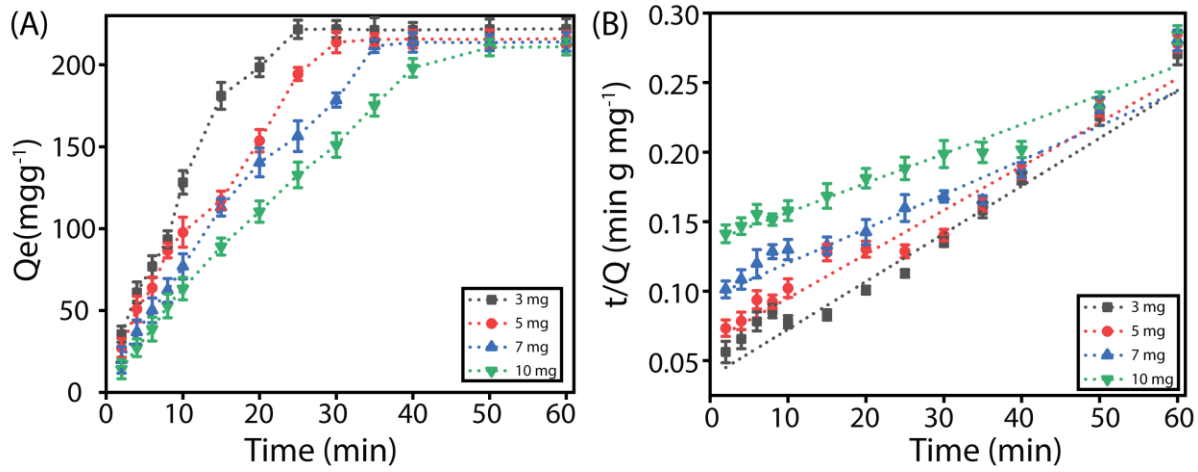

Fig. S22. Time-dependent desorption isotherm of phosphate ions by Zn-gCP polymer (3–10 mg) at pH 7.0 at room temperature (A), pseudo-second-order kinetics curves of phosphate desorption on Zn-gCP (3,5,7, and 10mg) at pH 7.0 under room temperature (B).

5.10. Advantages of Zn-gCP compared to other reported biomaterials — Zn-gCP, was synthesized via a three-step synthetic process. Initially, cellulose was modified with epichlorohydrin to produce the epoxy-functionalized compound **1**. Cellulose, being a biomaterial, does not pose any significant environmental impact. Epichlorohydrin, on the other hand, is widely used in water treatment processes for the preparation of ion-exchange resins and various bio-adsorbents. The primary product of this reaction is compound **1**, which serves as an intermediate for the synthesis of numerous water treatment adsorbents already documented in the literature. In the second step, the compound **1** reacted with 1-aminoguanidine, providing the guanidine-functionalized cellulose, gCP. 1-aminoguanidine is known for its various biomedical applications, including its antioxidant and antimicrobial properties, which could be advantageous for water disinfection. Finally, gCP reacted with Zn(II) salt (25% w/w) to produce the Zn-gCP polymer. Zinc is renowned for its antimicrobial properties and its strong affinity for phosphate ions. All the chemicals used for synthesizing the Zn-gCP polymer are environmentally friendly and highly cost-effective. In contrast, most reported biomaterials utilize lanthanide-based metal oxides and/ or zirconium-based metal oxides for phosphate removal from aqueous solutions, which are not only significantly more expensive but also pose severe environmental hazards as compared to zinc. Both the lanthanide

and zirconium-based metal ions are notably costlier and more toxic due to their lack of biological roles, environmental persistence, and interference with essential biological processes. The advantages of Zn-gCP over other reported biomaterials are discussed in detail, with parameters such as cost-effectiveness, environmental safety, and adsorption efficiency summarized in Table S3.

Table S3. Comparison of Zn-gCP polymer with recently reported biomaterials.

Sl No.	Compound	Adsorption Capacity (mg/g)	Equilibrium Time	Recycle	Cost-effectiveness	Environmental safety	Ref
1	Zn-gCP	310	20 min	0.5 N NaOH	Cost-effective and efficient compared to reported biomaterials.	Environmentally safe	This work
2	PAN_AF–Cl	15.49	5 min	0.3 mol L^{-1} HCl	Cost-effective but less efficient compared to Zn-gCP.	Environmentally safe	[3]
3	CMKGM-La microspheres	16.06	10 h	0.001 M NaOH	More costly than Zn-gCP	More environmentally harmful than Zn-gCP.	[4]
4	PAN-NH_2-Ce	17 mmol/g	24 h	0.1 M KNO_3, 0.1 M KOH	More costly than Zn-gCP	More environmentally harmful than Zn-gCP.	[5]
5	MALZ	80.8	180 min	0.5 M NaOH	More costly than Zn-gCP	More environmentally harmful than Zn-gCP.	[6]
6	La/GTB	109 ± 4	30 min	0.1 NaOH	More costly than Zn-gCP	More environmentally harmful than Zn-gCP.	[7]
7	MB	14.33 mg/m^2	120 min	NA	Cost-effective but less efficient compared to Zn-gCP.	Environmentally safe	[8]
8	CTS-Fe	15.7	48 h	0.5 M NaOH	Cost-effective but less efficient	Environmentally safe	[9]

					compared to Zn-gCP.		
9	Zirconium-modified zeolite	10.2	24 h	NA	More costly than Zn-gCP	More environmentally harmful than Zn-gCP.	[10]
10	PMSB800	25.19	24 h	NA	Cost-effective but less efficient compared to Zn-gCP.	Environmentally safe	[11]
11	Zr/Al-pillared montmorillonite	17.2	6 h	NA	More costly than Zn-gCP	More environmentally harmful than Zn-gCP.	[12]
12	Zr-loaded orange waste gel	57	15 h	95 % (0.2 M NaOH)	More costly than Zn-gCP	More environmentally harmful than Zn-gCP.	[13]
13	Zr-loaded wheat straw	31.9	10 h	98.2 % (5 wt % NaOH + 5 wt % NaCl)	More costly than Zn-gCP	More environmentally harmful than Zn-gCP.	[14]
14	ZrO_2-loaded amine crosslinked shaddock Peel	59.89	4 h	NA	More costly than Zn-gCP	More environmentally harmful than Zn-gCP.	[15]
15	Zr-modified activated sludge	27.55	270 min	0.1 mol L^{-1} NaOH	More costly than Zn-gCP	More environmentally harmful than Zn-gCP.	[16]
16	ZrO_2-loaded lignocellulose butanol residue	8.75	712 min	NA	More costly than Zn-gCP	More environmentally harmful than Zn-gCP.	[17]
17	La/C	48.8	NA	1 M NaOH	More costly than Zn-gCP	More environmentally harmful than Zn-gCP.	[18]

NA = Not Available.

5.11. Dynamic adsorption column experiment—

A glass column of diameter ~ 0.5 cm was packed with a mixture of 50 mg of the Zn-gCP polymer and 3 g of sand with a bed length ~ 5 cm for the dynamic adsorption column experiment. Initially, 50 mL of ultrapure milli-Q water was passed through the column bed to eliminate any bubbles present. After that, 500 mL of the 50-ppm aqueous phosphate solution, along with 2 times excess the amount of other anions (F^-, Cl^-, Br^-, NO_3^-, and SO_4^{2-}), was passed through the column bed with a flow rate of 0.5 mL/min following an equilibration time of 10 min. The eluents from the column were collected in 10 separate 50 mL batches, and the concentration of oxoanions in each batch was determined using IC. Observations revealed that up to 250 mL of the column eluent had phosphate concentrations lower than those recommended by the World Health Organization (WHO) in the first cycle. The column was rejuvenated by adding 100 mL of a NaOH (0.5 N) solution before moving on to the next cycle. Observations from the IC experiment revealed that over 93% of the phosphate was efficiently desorbed from the polymer through this procedure in the first cycle. The experiment was replicated up to 3 cycles, and the IC results consistently demonstrated that up to 200–250 mL of eluent from the column had phosphate concentrations below the WHO recommended threshold and efficiently removed over 85% of the phosphate from the Zn-gCP polymer after the third cycle (Fig. S23).

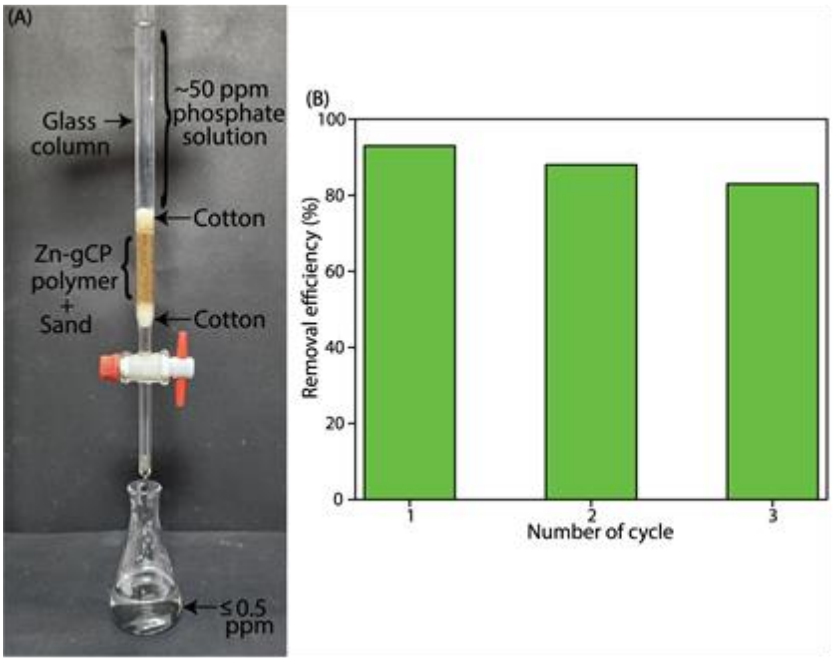

Fig. S23. Digital image for dynamic adsorption column experiment (A). Phosphate ions desorption efficiency (%) of Zn-gCP polymer in adsorption column experiment (B).

6. Antibacterial activities of the Zn-gCP polymer:

6.1. Microbicidal efficacy of the polymers — Antimicrobial activity of the polymers was tested against Gram-negative (*Escherichia coli*, MTCC 1687) and Gram-positive (*Staphylococcus aureus*, MTCC 96) bacteria. Glycerol stock of the bacterial strain was cultured onto agar media supplemented with Luria Bertani (LB) nutrient media at 37 °C. A single colony of the bacterial strain was cultured in broth media and grown till mid logarithmic phase in a shaker incubator at 37 °C, 180 rpm. The stock solution of the polymer was prepared in Milli-Q water with a concentration of 500 µg/mL for *Staphylococcus aureus* and 1500 µg/mL for *Escherichia coli*. The solution was then subjected to sonication and subsequently underwent serial dilution in a 96-well plate. The solution exhibits a reddish-brown colour, which can be attributed to the inherent colouration of the polymer (gCP in A, Zn-gCP in B, and Zn-gCP-P in C), which eventually diminished with a dilution of the polymer solution. Bacterial culture was harvested by centrifugation and added to the 96-well plate containing the serially diluted polymers at 10^6 CFU/mL. The plate was incubated at 37 °C for 4 to 6 h. After that, 10 µL polymer treated culture was transferred to the fresh broth media (A to A′ in case of gCP polymer, B to B′ in case of Zn-gCP polymer, C to C′ in case of Zn-gCP-P polymer, and D to D′ in case of unmodified cellulose polymer), and the plate was again incubated at 37 °C for 14 to 16 h. Due to the transfer of only 10 µL into the fresh media (190 µL), the media did not acquire the colouration of the compound as observed in the A′ (gCP), B′ (ZN-gCP), and C′ (Zn-gCP-P) samples. The bacterial growth was visually observed or measuring the optical density at 600 nm. The experimental results demonstrated that at a 250 µg/mL concentration, the gCP polymer showed bactericidal activity against *S. aureus*. In comparison, at 125 µg/mL concentration, both the Zn-gCP and Zn-gCP-P polymers indicated bactericidal activity against *S. aureus*. The gCP polymer displayed bactericidal activity against *E. coli* at 375 µg/mL, whereas the Zn-gCP and Zn-gCP-P polymers did so at a concentration of 187.5 µg/mL. However, it was evident from the experiment that unmodified cellulose did not exhibit bactericidal activity against both *S. aureus* and *E. coli*.[19, 20]

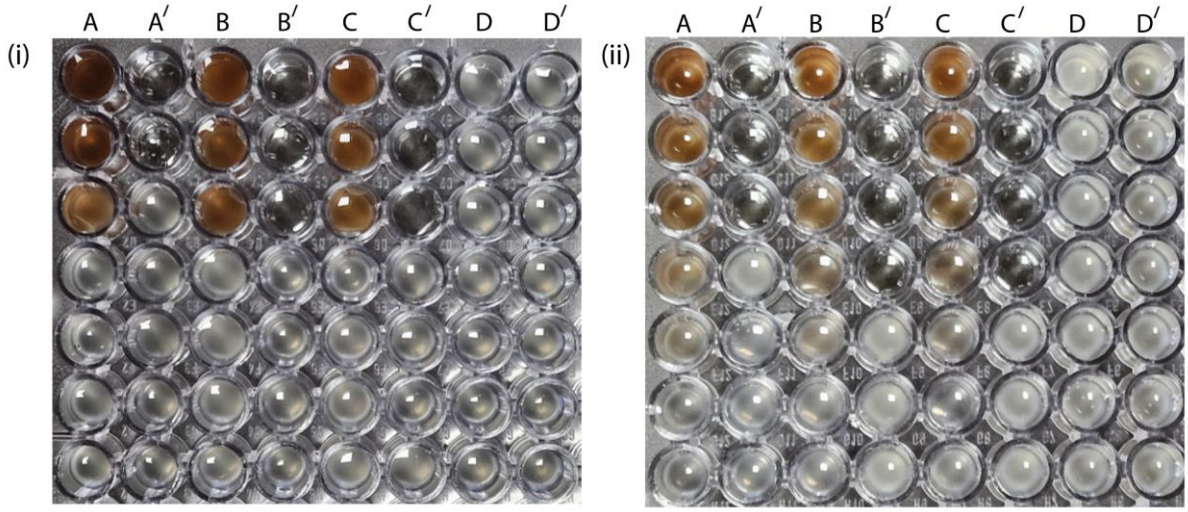

Fig. S24. Bactericidal activity of the polymers (gCP, Zn-gCP, ZN-gCP-P, and unmodified cellulose) against *S. aureus* (i) and *E. coli* (ii). A, B, C, and D in the figure represent gCP, Zn-gCP, Zn-gCP-P, and unmodified cellulose, respectively, in the initial antibacterial study. Whereas A′, B′, C′, and D′ represent the same after transferring the 10 μL of the compounds from A, B, C, and D, respectively, in fresh media for further study.

6.2. Morphological analysis of the polymer-treated bacterial cells — The *S. aureus* bacterial cells were cultured as mentioned in the above section. Bacterial cells were treated with the polymers and incubated at 37 °C, 180 rpm. Cells were harvested by centrifugation and suspended in the buffer. Cells were fixed with 3 % glutaraldehyde and kept for 30 min washed with Milli-Q, and mounted onto to glass grid. After drying the sample under laminar airflow, it was stacked onto a FESEM grid and coated with gold. Morphology was analysed at different magnifications under the microscope.

6.3. Microbicidal activity against real water sample — To analyze the application of microbicidal polymer the water sample was collected from IITG lake and treated with the polymers at a concentration of 0.25 mg/mL. For control water sample without treatment was also taken, and all the samples were shaken for 6 h at room temperature. Water samples were plated onto agar nutrient LB media, and the plate was incubated for 16 to 20 h at 37 °C. The growth of the microbes was analyzed on the plate after the incubation.

7. References:

1. X. Ye, A. Wang, D. Zhang, P. Zhou and P. Zhu, Light and pH dual-responsive spiropyran-based cellulose nanocrystals, *RSC Adv.*, 2023, **13**, 11495-11502.

2. X. Ye, H. Wang, L. Yu and J. Zhou, Aggregation-induced emission (AIE)-labeled cellulose nanocrystals for the detection of nitrophenolic explosives in aqueous solutions, *Nanomaterials*, 2019, **9**, 707.
3. W. Zheng, Q. Wu, W. Xu, Q. Xiong, Y. K. Kalkhajeh, C. Zhang, G. Xu, W. Zhang, X. Ye and H. Gao, Efficient capture of phosphate from wastewater by a recyclable ionic liquid functionalized polyacrylonitrile fiber: A typical "release and catch" mechanism, *Environ. Sci. Water Res. Technol.* , 2022, **8**, 607-618.
4. X. Zhang, X. Lin, Y. He, Y. Chen, J. Zhou and X. Luo, Adsorption of phosphorus from slaughterhouse wastewater by carboxymethyl konjac glucomannan loaded with lanthanum, *Int. J. Biol. Macromol.*, 2018, **119**, 105-115.
5. Y. G. Ko, T. Do, Y. Chun, C. H. Kim, U. S. Choi and J.-Y. Kim, CeO2-covered nanofiber for highly efficient removal of phosphorus from aqueous solution, *J. Hazard. Mater.*, 2016, **307**, 91-98.
6. W. Shi, Y. Fu, W. Jiang, Y. Ye, J. Kang, D. Liu, Y. Ren, D. Li, C. Luo and Z. Xu, Enhanced phosphate removal by zeolite loaded with Mg–Al–La ternary (hydr) oxides from aqueous solutions: performance and mechanism, *J. Chem. Eng.*, 2019, **357**, 33-44.
7. Y. Huang, X. Lee, M. Grattieri, M. Yuan, R. Cai, F. C. Macazo and S. D. Minteer, Modified biochar for phosphate adsorption in environmentally relevant conditions, *J. Chem. Eng.*, 2020, **380**, 122375.
8. M. El Bouraie and A. A. Masoud, Adsorption of phosphate ions from aqueous solution by modified bentonite with magnesium hydroxide Mg (OH) 2, *Appl. Clay Sci.*, 2017, **140**, 157-164.
9. Z. B. Zhang BoaiQi, C. N. Chen Nan, F. C. Feng ChuanPing and Z. Z. Zhang ZhenYa, Adsorption for phosphate by crosslinked/non-crosslinked-chitosan-Fe (III) complex sorbents: characteristic and mechanism, *J. Chem. Eng.*, 2018.
10. M. Yang, J. Lin, Y. Zhan, Z. Zhu and H. Zhang, Immobilization of phosphorus from water and sediment using zirconium-modified zeolites, *Environ. Sci. Pollut.*, 2015, **22**, 3606-3619.
11. M. Zhang, K. Lin, X. Li, L. Wu, J. Yu, S. Cao, D. Zhang, L. Xu, S. J. Parikh and Y. S. J. E. P. Ok, Removal of phosphate from water by paper mill sludge biochar, *Environ. Pollut.* , 2022, **293**, 118521.
12. J. Chen, L.-g. Yan, H.-q. Yu, S. Li, L.-l. Qin, G.-q. Liu, Y.-f. Li and B. Du, Efficient removal of phosphate by facile prepared magnetic diatomite and illite clay from aqueous solution, *Appl. Clay. Sci.*, 2016, **287**, 162-172.
13. B. K. Biswas, K. Inoue, K. N. Ghimire, H. Harada, K. Ohto and H. Kawakita, Removal and recovery of phosphorus from water by means of adsorption onto orange waste gel loaded with zirconium, *Bioresource Technol.*, 2008, **99**, 8685-8690.
14. H. Qiu, C. Liang, J. Yu, Q. Zhang, M. Song and F. Chen, Preferable phosphate sequestration by nano-La (III)(hydr) oxides modified wheat straw with excellent properties in regeneration, *Acs Appl. Mater. Inter.*, 2017, **315**, 345-354.
15. P. Duan, X. Xu, Y. Shang, B. Gao and F. Li, Amine-crosslinked Shaddock Peel embedded with hydrous zirconium oxide nano-particles for selective phosphate removal in competitive condition, *Taiwan Inst. Chem. E*, 2017, **80**, 650-662.
16. J. Wang, X. Tong and S. Wang, Zirconium-modified activated sludge as a low-cost adsorbent for phosphate removal in aqueous solution, *Water Air Soil Pollut.*, 2018, **229**, 1-10.
17. E. Zong, X. Liu, J. Jiang, S. Fu and F. Chu, Preparation and characterization of zirconia-loaded lignocellulosic butanol residue as a biosorbent for phosphate removal from aqueous solution, *Appl. Surf. Sci.*, 2016, **387**, 419-430.

18. W.-J. Xia, L.-X. Guo, L.-Q. Yu, Q. Zhang, J.-R. Xiong, X.-Y. Zhu, X.-C. Wang, B.-C. Huang and R.-C. Jin, Phosphorus removal from diluted wastewaters using a La/C nanocomposite-doped membrane with adsorption-filtration dual functions, *J. Chem. Eng.*, 2021, **405**, 126924.
19. S.-W. Zhao, C.-R. Guo, Y.-Z. Hu, Y.-R. Guo and Q.-J. Pan, The preparation and antibacterial activity of cellulose/ZnO composite: A review, *A review. Open Chem.*, 2018, **16**, 9-20.
20. M. N. F. Norrrahim, N. M. Nurazzi, M. A. Jenol, M. A. A. Farid, N. Janudin, F. A. Ujang, T. A. T. Yasim-Anuar, S. U. F. S. Najmuddin and R. A. Ilyas, Emerging development of nanocellulose as an antimicrobial material: An overview, *An overview. Mater. Adv.*, 2021, **2**, 3538-3551.